nature communications

Article

https://doi.org/10.1038/s41467-025-58103-y

Large scale submarine groundwater discharge dominates nutrient inputs to China's coast

Received: 24 December 2024

Accepted: 12 March 2025

Published online: 25 March 2025

Check for updates

Tianyi Zhu[1,2,3,4], Shibin Zhao[1,2], Bochao Xu[1,2] ✉, Dongyan Liu[5], M. Bayani Cardenas[6], Huaming Yu[7,8], Yan Zhang[9], Xiaogang Chen[10], Kai Xiao[11], Lixin Yi[12], Hyung-Mi Cho[13], Sumei Liu[1,14], Ziliang Zhang[7,8], Ergang Lian[15,16], William C. Burnett[17], Guangquan Chen[18], Zhigang Yu[1,2] ✉ & Isaac R. Santos[19]

Submarine groundwater discharge (SGD) is a nutrient source to coastal waters. However, most SGD estimates are restricted to a local scale and hardly distinguish contributions from fresh (FSGD) and recirculated (RSGD) SGD. Here, we compiled data on radium/radon of groundwater (n ~ 2000) and seawater (n ~ 10,000) samples along ~18,000 km of China's coastal seas to resolve large scale FSGD and RSGD and their associated nutrient loads. Nearshore-scale FSGD (~ 3.56×10^8 m^3 d^{-1}) was only 2% of the total SGD but comparable to RSGD in terms of nutrient loads. Despite large uncertainties quantified via Monte Carlo simulations, SGD was a dominant contributor to China's coastal nutrient budgets, with dissolved inorganic nitrogen, phosphorus and silicate fluxes of ~395, 2.9, and 581 Gmol a^{-1}, respectively. Total SGD accounted for 19–54% of nutrient inputs, exceeding inputs from atmospheric deposition and rivers. Overall, SGD helps sustaining primary production along one of the most human-impacted marginal seas on Earth.

Submarine groundwater discharge (SGD) pertains to all flow from the seabed to the coastal waters along continental margins regardless of salinity or driving force[1–3]. Fresh SGD (FSGD) represents terrestrial groundwater flow driven primarily by hydraulic gradients[4,5], whereas recirculated SGD (RSGD) represents brackish groundwater or seawater circulating through sediments[6,7]. Local-scale SGD has been widely quantified through application of radium and radon isotopes, because of their large enrichment in groundwater relative to seawater[8–10]. The combination of multiple isotopes with different half-lives allows for tracing different SGD pathways[9]. While most investigations have resolved SGD at the local (several to tens of kilometers) and regional (tens to hundreds of kilometers) scales, continental scale assessments over hundreds of kilometers are essential for minimizing site-selection biases and resolving the net contribution of SGD to coastal ocean budgets[6].

SGD transports large amounts of nutrients[11], heavy metals[12], organic matter[6], carbon dioxide[13], and other chemical compounds to the ocean. Nutrients, including dissolved inorganic nitrogen (DIN), dissolved inorganic phosphorus (DIP), and dissolved inorganic silicate (DSi), fuel primary production and food webs. Rapidly increasing excess nutrient inputs from land-based sources often lead to severe eutrophication in coastal waters in China and elsewhere[14,15]. While river fluxes have been widely monitored[16] and long-term trends are now available[17], SGD is either neglected due to a lack of local data[18,19] or dismissed due to uncertainties[20,21] in large scale studies. A comprehensive assessment of SGD impacts on nutrient budgets is needed to resolve whether SGD is an important driver of coastal eutrophication[6].

The large global marginal seas usually have high productivity and are exposed to great pressure from human activities[22,23]. Many

A full list of affiliations appears at the end of the paper. ✉e-mail: xubc@ouc.edu.cn; zhigangyu@ouc.edu.cn

local-scale studies have quantified SGD in China's bays, estuaries, continental shelves[24], and marginal seas[25]. A literature compilation suggested that median SGD fluxes are ~6 cm d^{-1} in China's coastal waters[24]. A bottom-up upscaling of these local-scale study cases led to the conclusion that SGD may exceed river fluxes to China's continental shelf. However, the many unique study cases may have targeted areas of special interest and potentially high SGD. Large scale observations and models covering the entire coastline are needed to prevent spatial biases and potentially over- or under-estimate SGD contributions.

Existing global and ocean basin SGD assessments have relied on radium mass balances[7] or hydrological models[5] without separating FSGD from RSGD. FSGD typically represents a relatively small volume of water and new nutrients to the ocean, while RSGD seems to be an important nutrient recycling pathway[1,26,27]. With highly polluted coastal aquifers leading to high concentrations of nutrients[15], the contribution of FSGD to developed coastlines may be particularly important[5]. Widespread nutrient-driven coastal eutrophication enhances phytoplankton biomass, providing organic matter that may eventually be decomposed within sediments and returned to the ocean via RSGD. Resolving the relative contribution of FSGD and RSGD is thus essential for understanding the magnitude of SGD's contribution to nutrient budgets.

Here, we first build an extensive compilation of > 10,000 radium and radon data over ~18,000 km of China's coastline extending to more than 500 km offshore (Fig. 1). This allows us to zoom out from local hotspots to provide unbiased large-scale estimates of FSGD and RSGD and their associated nutrient fluxes. To put SGD fluxes in perspective, we construct comprehensive large-scale nutrient budgets without biases towards areas of known SGD or river inputs. Our results contribute to the protection and management of marginal seas under high pressure from China's burgeoning economy and a coastal population exceeding 260 million[28].

Results and discussion

Radium and radon enrichments in nearshore waters

The distributions of surface water ^{222}Rn, ^{224}Ra, ^{226}Ra, and ^{228}Ra activities generally decreased offshore (Fig. 2), revealing a dominant nearshore source. Owing to different decay rates, the short-lived ^{222}Rn and ^{224}Ra isotopes decline from nearshore highs to values approaching zero at ~0–50 km from the shoreline, while the long-lived ^{226}Ra and ^{228}Ra approach stable asymptotic values near the shelf break at ~100–500 km from the shoreline. The highest SGD tracer activities were found in the enclosed Bohai Sea, followed by the Yellow Sea, East China Sea, and South China Sea. Residence times in the Bohai Sea (3.4 years) and Yellow Sea (~3.8–11.8 years) are longer due to their semi-enclosed shape[29–31], allowing for long-lived isotope accumulation. The lower concentrations on shelves of the East and South China Seas are a reflection of the much shorter residence times (< 1 year) due to effective mixing with open Pacific Ocean[29,32].

The high nearshore activity of radium and radon originates from SGD, sediment diffusion and terrestrial runoff. The three large river delta-front estuaries release solutes to the coastal ocean. Local scale SGD fluxes may exceed river discharge in some cases, leading to high activities of radium or radon, and driving algal blooms[33,34]. Abundant animal burrows promoting porewater exchange in waters adjacent to mangroves and saltmarshes[35,36], and large tidal ranges (~3–6 m in some cases) enhance SGD and short-lived isotope concentrations in nearshore waters[37]. The contribution of sediment diffusion to Ra and Rn in seawater is similar to or even surpasses SGD and river inputs in some local areas, such as the Pearl River Estuary in the wet season and Bohai Bay[34,38] but it is expected to be smaller than SGD when considering large scale budgets[7]. Both Ra and Rn exhibit slightly higher activities in autumn (Supplementary Fig. 1) possibly from lagged inputs following the rainy season[4,6].

Highly variable groundwater endmembers

There is substantial heterogeneity in groundwater endmember Ra and Rn concentrations. Salinity best explained this large spatial variability (Supplementary Fig. 2). The median radium activity in brackish groundwater was 14 (short-lived ^{224}Ra) and 3 to 4 (long-lived ^{228}Ra and ^{226}Ra) times greater than that in fresh groundwater. In contrast, the median ^{222}Rn activity in fresh groundwater was 3 times greater than that in brackish groundwater. The contrasting salinity gradients allow for the use of isotope combinations to separate the relative contributions of fresh and recirculated SGD (see Supplementary Note 1). Fresh groundwater samples with salinities ≤ 1 were defined as groundwater endmembers for FSGD. Radium in fresh water is strongly adsorbed onto particles and thus highly insoluble[39]. Brackish conditions (salinities > 1) release radium from particles, dramatically increasing radium concentrations in groundwater[40,41]. Hence, radium isotopes primarily trace the dominant RSGD signal.

The contribution of salinity to the distribution of Ra and ^{222}Rn in groundwater exceeded the contribution of other factors such as seasons, sediment types and basins (Supplementary Fig. 3). There were no detectable seasonal variations (Supplementary Fig. 3a–d). Our observations revealed comparable median values across sandy, muddy, and mixed sediments, preventing the use of sediment types to distinguish groundwater endmembers (Supplementary Fig. 3e–h). The ~18,000 km China's coastlines can be divided into four major basins (Bohai, Yellow, East and South China) that had no clear spatial differences of Ra or ^{222}Rn (Supplementary Fig. 3i–l). The local scale isotope production in coastal aquifers is also related to sediment composition and residence time of groundwater, but these drivers are not apparent from our large China coast scale[42,43].

Small fresh and large recirculated SGD

Multi-scale FSGD and RSGD fluxes and uncertainties were estimated using Monte Carlo simulations assuming all terms followed either a normal or lognormal distribution[44], as indicated by empirical data distributions. The mean and standard deviations are reported if a parameter or result is normally distributed; while the quartiles (25^{th}, 50^{th}, and 75^{th} quantiles) are presented when lognormally distributed. The fluxes of nearshore-scale FSGD and RSGD were highly variable at 0.16 ± 7.06 and 7.95 (2.38–19.6) cm d^{-1} (Supplementary Table 1, Fig. 3b) due to the large sampling heterogeneity. These SGD fluxes upscaled to volumes were (3.56 ± 161) × 10^8 and 182 (54–448) × 10^8 m^3 d^{-1}, that were ~0.09 and 4.61 times the total freshwater river flux draining into China's coastal seas (3.95 × 10^9 m^3 d^{-1}, Supplementary Table 2). The large contribution of RSGD (~ 98% of the total SGD) on the China-coast scale is consistent with other ^{228}Ra budgets calculated for large ocean basins (~95% in the Mediterranean Sea)[10] and local-scale investigations in China (~93% and 95–98% in the Yellow Sea and the Bohai Sea, respectively)[45–47]. Our small FSGD fluxes are also consistent with earlier suggestions that FSGD accounts for less than 10% of total SGD in global coastal locations[48].

The shelf-scale RSGD was estimated utilizing ^{226}Ra and ^{228}Ra to be 2.3 (0.9–5.2) cm d^{-1} or 2.1 (0.8–4.8) × 10^{10} m^3 d^{-1} (Supplementary Table 1, Fig. 3b). The nearshore-scale RSGD rates were 3.5 times greater than the total shelf-scale RSGD. Hence, ~87% of the RSGD flux off China occurs in nearshore shelf waters with short residence times (< 20 d) and/or shallow depths (< 30 m). Our estimates of total SGD in the China's coastal seas are in line with that in the Eastern China Marginal Seas (1.2 ± 0.8 cm d^{-1}) and the estimates based on previous local-scale SGD rates (1.1–2.2 cm d^{-1})[24,25] (Supplementary Table 3). The total SGD flux along China's coastal seas is about 6% of the global total SGD estimate ((3.3 ± 0.8) × 10^{11} m^3 d^{-1}) with similar rates, which was about 16 and 3 times greater than that of the Mediterranean Sea (0.2 (0.0–0.5) cm d^{-1}) and the Atlantic Ocean (0.6–1.2 cm d^{-1})[7,10,49].

The occurrence of FSGD on continental shelves has been described globally using salinity or other geochemical, geophysical, and

https://doi.org/10.1038/s41467-025-58103-y

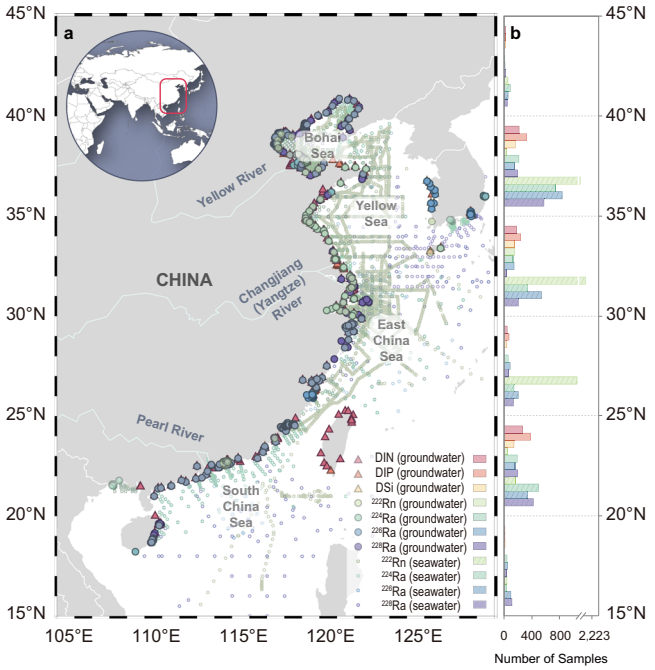

Fig. 1 | Locations of compiled groundwater and seawater samples along China's ~18,000 km coastline. a All sampling sites. Solid triangles and circles represent nutrients and isotopic measurements in groundwater, respectively. Open circles represent Ra or Rn sample sites in seawaters. The sampling sites for dissolved inorganic nitrogen (DIN), dissolved inorganic phosphorus (DIP), dissolved inorganic silicate (DSi), ^{222}Rn, ^{224}Ra, ^{226}Ra, and ^{228}Ra are denoted by red, orange, yellow, green, cyan, blue, and purple colors, respectively. **b** The frequency of different types of samples with latitude. Source data are provided as a Source Data file in Supplementary Data 1. The map of panel a is generated with Ocean Data View (https://odv.awi.de).

modelling approaches[50,51], yet no large-scale flux estimates are presently available. Typically, FSGD is only a minor proportion of total SGD on local to global scales[10,48]. FSGD mainly occurs in nearshore areas unless there are karst or volcanic aquifers directly connecting terrestrial aquifers to the continental shelf[6]. Our mass balance approach revealed that nearshore scale FSGD was only 2% of RSGD. This minor contribution, the lack of detectable offshore freshening, and the absence of large karst or volcanic aquifers off China implies that FSGD is small or negligible on this shelf. Both ^{226}Ra and ^{228}Ra were highly enriched in brackish groundwater compared to fresh groundwater. Hence, the radium signal would not be strong enough to detect small fresh SGD inputs offshore.

SGD served as the primary source of Ra and ^{222}Rn within the study area, accounting for 80–90% of the total sources in the mass balances (Supplementary Table 4). Uncertainties induced by various input terms were obtained from Monte Carlo simulations (Supplementary Note 1). The wide distributions highlight inherent uncertainties that are poorly understood. As in most local scale SGD studies, groundwater endmembers are the most significant source of uncertainties[52,53]. Our wide spatial coverage and large sample size creates a wide range of potential endmembers that leads to large uncertanties[37]. We assumed a groundwater endmember from its lognormal distribution as advocated by others to minimize the impact of outliers[7,26]. The lognormal standard deviation exceeded lognormal mean values, especially for short-lived isotopes. The Monte Carlo simulations imply that negative FSGD are a possible outcome of our modelling exercise. However, negative FSGD rates are physically impossible and represent an artefact of large endmember uncertainties. Mixing between nearshore and offshore waters contributed 90–100% of all sinks of ^{226}Ra and ^{228}Ra and 20–30% to that of ^{224}Ra and ^{222}Rn, representing a large source of uncertainty. Residence time uncertainties range from 50 to 100% in the shelf region and 70 to 130% in the nearshore region due to the seasonality of ocean currents (Supplementary Note 1).

Large impact of SGD on nutrient inputs

Our widespread groundwater nutrient sampling covers many coastal ecosystems, climates, and geological feature. Relatively high concentrations of nutrients and DIN:DIP and DSi:DIP ratios in groundwater were observed in the highly-developed regions near the Changjiang River Estuary and the Pearl River Estuary (Supplementary Fig. 4), where urbanization levels are extreme[54,55]. However, we note no simple correlation between urbanization levels and groundwater nutrient concentrations. There was no seasonal variation observed in DIN and DIP in groundwater, while the concentration of DSi was 2–4 times higher in summer and autumn than in spring and winter (Supplementary Fig. 5).

Nutrient concentrations decreased with increasing salinity (Supplementary Fig. 6). The median concentrations of nutrients in fresh groundwater (salinity ≤1) were 1.3–5.5 times greater than in groundwater with salinity >1. Median dissolved nutrients in all groundwater samples were 0.5–1 times relative to that in river, but 1.1–3.4 times more enriched than seawater, indicating a potential impact of SGD-derived nutrients into coastal seawaters. For FSGD, nutrient fluxes were calculated by multiplying fresh groundwater concentrations with FSGD fluxes. The difference of nutrient concentrations between brackish groundwater and seawater was used for the calculation of RSGD-derived nutrient fluxes to remove the effect of nutrients originally present in seawater infiltrating coastal aquifers.

The nutrient loads by total SGD were ~395, 2.9, 581 Gmol a^{-1}, exceeding river input by 2.7, 2.1 and 5.1 times respectively for DIN, DIP, and DSi (Supplementary Table 5). Even though FSGD accounted for a small part of the total SGD (~ 2%), its nutrient contributions made up 50%, 25% and 52% of the total SGD-derived DIN, DIP and DSi, respectively. Dissolved nutrients in recirculated groundwater exchanged with seawater, but still represent a significant net source. Our China-scale total SGD-derived nutrients are comparable with that derived from local estimates, and accounted for 7%, 2%, and 15% of the total input of DIN, DIP, and DSi from global SGD (Supplementary Table 3)[11,24,26]. China's marginal seas, that cover only 4% of the global shoreline are thus hotspots of SGD transporting nutrients to the oceans. Excess nutrients derived by SGD will contribute to several major environmental issues in China's coastal waters, including eutrophication and harmful algae blooms (HABs)[56,57]. HABs often occur in large river estuaries and semi-enclosed bays[58]. High-values of Ra and ^{222}Rn in seawaters (Fig. 2) and nutrients in groundwater endmembers (Supplementary Fig. 4) have similar distribution patterns as HABs[58], implying a link between higher inputs of SGD-derived nutrients and HABs. However, establishing a large-scale link between HABs and SGD remains challenging due to the episodic nature of most algal blooms and the spatially-integrated nature of our isotope mass balance models.

To put SGD fluxes in perspective, we developed nutrient budgets for the entire China shelf (Fig. 3a, c; Supplementary Table 6; Supplementary Note 2). Out of all external sources, SGD accounted for 32%, 19%, and 54% of DIN, DIP, and DSi, respectively. SGD-derived nutrients exceeded those from rivers and atmospheric deposition and were comparable to benthic diffusion, contributing 2–25% to the regional primary production. Our estimated total SGD contributions exceed previous estimates in the Yellow and Bohai Sea at 1–7% for nutrients[20,59]; and 18% for DSi in the South China Sea[60]. Hence, our estimates show that differences in multi-scale SGD should be considered in nutrient budgets.

The total shelf sinks of DIN, DIP and DSi were 1350 ± 262, 47 ± 2 and 967 ± 196 Gmol a^{-1}, and the total sources were 1230 ± 193, 15 ± 1, 1030 ± 79 Gmol a^{-1}. The DIN and DSi budgets are roughly in balance,

https://doi.org/10.1038/s41467-025-58103-y

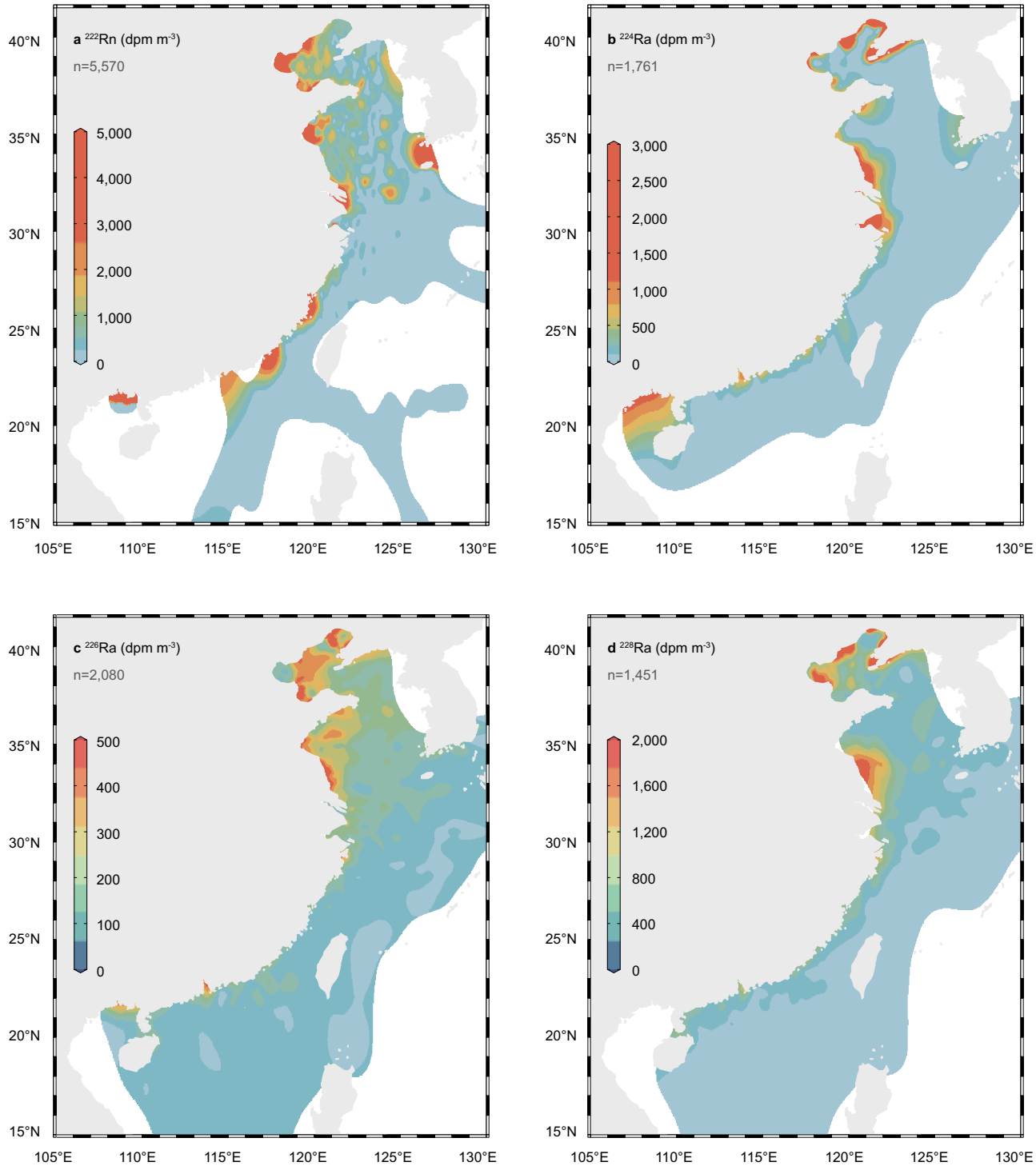

Fig. 2 | The spatial distribution of four submarine groundwater discharge (SGD) tracers in China's coastal surface waters. The four tracers include ^{222}Rn (**a**), ^{224}Ra (**b**), ^{226}Ra (**c**), and ^{228}Ra (**d**). Source data are provided as a Source Data file in Supplementary Data 1. The maps are generated with Ocean Data View (https://odv.awi.de).

whereas the DIP budget is unbalanced with a missing source of 32 ± 2 Gmol a^{-1}. Particles are the major external P source at 23 Gmol a^{-1} in the Bohai and Yellow Sea[59]. Thus, unquantified adsorption/desorption cycles and weathering may explain the P budget deficit[61,62]. SGD-derived dissolved organic nitrogen and phosphorus remain as unquantified sources that warrant further investigation[63].

Ratios of nutrients in groundwater substantially differ from Redfield ratios (N:P:Si=16:1:15). The N/P/Si ratios of FSGD (272/1/415) deviates from benthic diffusion (117/1/54), river water (107/1/82) and RSGD (92/1/130) (Fig. 3). A greater proportion (~62%) of groundwater samples were enriched in DIN than river water (~43%) (Fig.4). Relatively high N:P ratios in groundwater result from wastewater, fertilizer, and preferential adsorption of PO_4 onto sediment grains[11]. Most of China's coastal waters are P-limited or are trending towards P limitation due to large N inputs[64,65], with smaller N:P (~ 39 and 20 in the Bohai and Yellow Seas) and similar N:Si (~0.6 and 1 in the Bohai and Yellow Seas) compared with groundwater[14,46]. SGD inputs will lead to an even greater P deficiency. High N:P ratios in groundwater increase the risk of harmful

https://doi.org/10.1038/s41467-025-58103-y

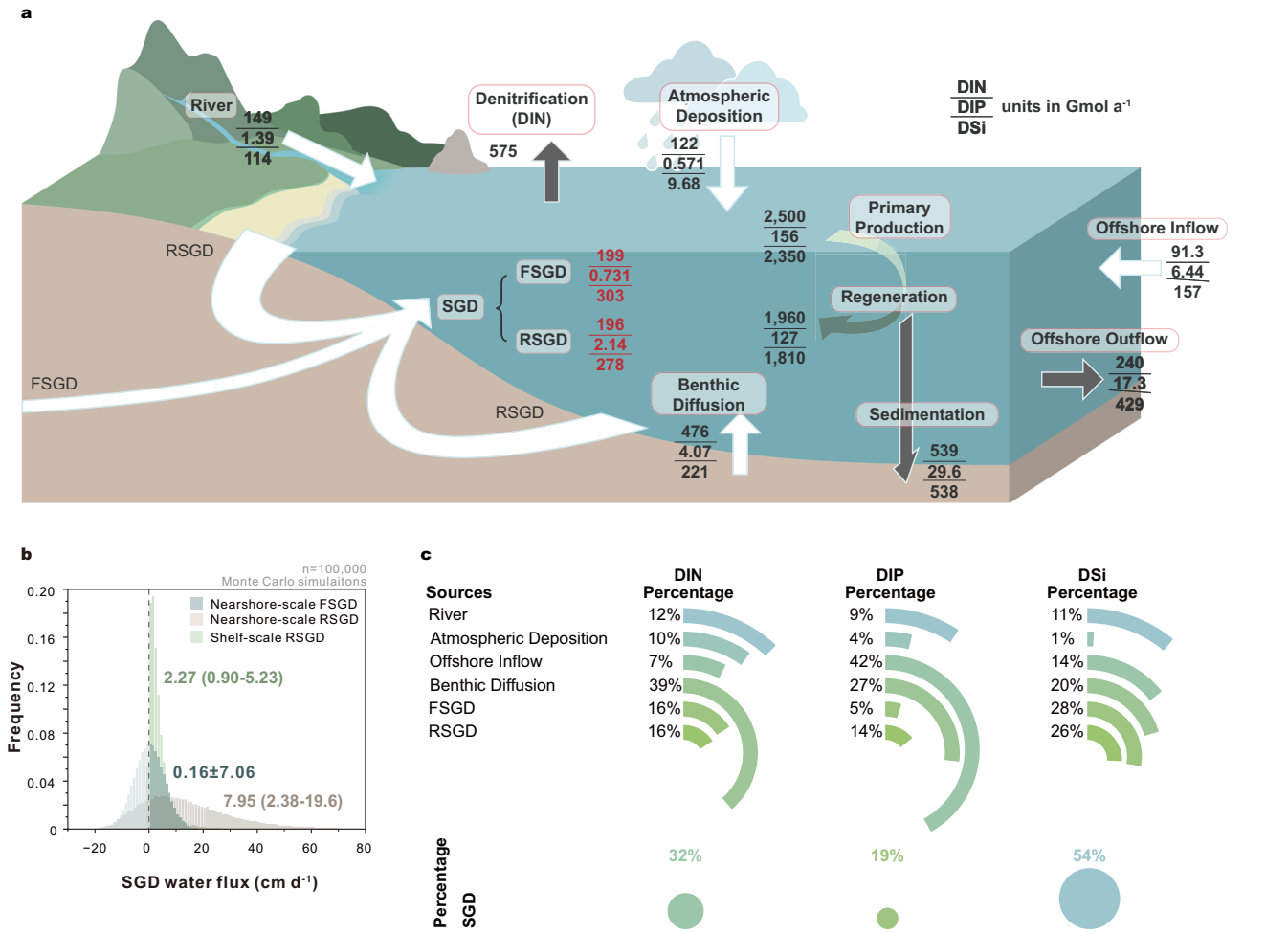

Fig. 3 | The contributions of submarine groundwater discharge (SGD) to nutrients budgets along China's continental shelf. a Dissolved inorganic nitrogen (DIN), dissolved inorganic phosphorus (DIP), and dissolved inorganic silicate (DSi) budgets in China's continental shelf including SGD's contribution excluding the undersampled Southern South China Sea. All fluxes are in Gmol a^{-1}. SGD is composed of fresh SGD (FSGD) and recirculated SGD (RSGD). The sedimentation of nitrogen (N), phosphorus (P), and silica (Si) are in forms of organic nitrogen (ON), organic phosphorus (OP), and biogenic silica (BSi). The white, black, and green arrows denote the inflow, outflow, and internal cycling of nutrients within the system, respectively. Details can be found in Supplementary Note 2. **b** Synthetic probability distribution functions (pdfs) of the multi-scale SGD water flux calculations conducted with the 10,000 input values (i.e., Monte Carlo simulations). The data accompanying each histogram represent the SGD water flux (the mean and standard deviation or 25th, 50th, and 75th quantiles) with the unit of cm d^{-1}. The *Y* axis is normalized frequency. **c** Percentages of external nutrient sources to China's coastal waters.

algal blooms (usually dinoflagellates)[57], and low N:Si ratios encourage diatom growth[66]. Hence, SGD is not only an essential source of nutrients, but also an important factor controlling nutrient ratios and potentially phytoplankton community composition. Previous observations revealed increasing DIN:DIP ratios in China's coastal seas as a response to both SGD and river inputs[14,24]. The large fluxes and imbalanced nutrient stoichiometry make SGD important in management plans designed to reduce eutrophication. Long-term observations of coastal groundwater and SGD should become routine for monitoring programs.

We resolved combined isotope budgets to address large scale FSGD and RSGD along China's continental shelf. SGD transported large amounts of nutrients and regulated the composition of seawater. The contribution of total SGD to nutrients was the largest among all external sources. Both FSGD and RSGD will exacerbate P-limitation due to high N:P ratios and stimulate the growth of phytoplankton groups adapted to high N conditions. FSGD constituted only 2% of the total SGD fluxes, but it made up 25–52% of the total SGD-derived nutrients. Monte Carlo simulations revealed persistent uncertainties mainly due to large natural variability of the groundwater endmember. Recognizing these large uncertainties is essential for interpreting nutrient budgets and predicting the impact of SGD on coastal biogeochemistry. Our estimate of large-scale SGD builds on many earlier local-scale studies suggesting a major impact of hidden SGD pathways to coastal biogeochemistry and nutrient budgets. Our results improve the understanding of water and nutrient cycles in one of the most impacted marine regions on Earth receiving inputs from >1.4 billion people.

Methods

Data sources

Radium, radon and nutrient observations acquired over several years were first collated and synthesized from both published and unpublished sources. We searched for data using Web of Science (Thomson Reuters, New York, NY) and Baidu Scholar with key words such as submarine groundwater discharge; and radium or radon with China and sea/groundwater/river. To determine the nutrient endmember concentration in SGD, we also compiled coastal groundwater nutrient data from the literature and by contacting the community of SGD researchers (Fig. 1). Detailed information about sample collection and

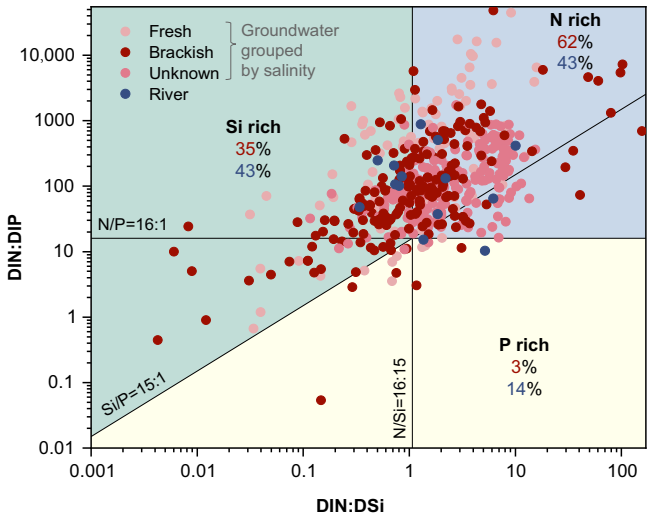

Fig. 4 | DIN:DIP (the ratios of dissolved inorganic nitrogen to phosphorus) and DIN:DSi (the ratios of dissolved inorganic nitrogen to silicate) in submarine groundwater discharge (SGD) and river[16,52,69,70] constituents along the coastlines. Dots and texts in red or blue represent groundwater or river. Blue, yellow, and green areas indicate water enriched in DIN, DIP, and DSi, respectively. Most groundwater samples are enriched in DIN and DSi. Hence, SGD will further push China's shelf waters towards P limitation. Source data are provided as a Source Data file in Supplementary Data 1.

analysis can be found in Supplementary Note 3. References with all data are presented in Supplementary Data 1. Water depths were retrieved from the ocean bathymetry database (https://www.ngdc.noaa.gov/mgg/global/global.html). As one of the most studied coastlines on Earth, we compiled a comprehensive dataset with ~10,000 lines of radium and radon activities in surface seawater, and more than 2000 in coastal groundwater along the ~18,000 km coastline of China (Fig. 1).

Estimating multi-scale SGD

Multi-tracer mass balance models were constructed to estimate SGD fluxes using ^{224}Ra, ^{226}Ra, ^{228}Ra and ^{222}Rn observations in seawater. The model was built under the assumption of steady state for two regions (Supplementary Fig. 7). The nearshore region (inner shelf) extends from the shoreline to where short-lived radium and radon isotopes approach zero. The nearshore region is an SGD hotspot with short water residence times (< 20 days), and/or shallow water depth (< 30 m). The shelf region extends to where the concentration of long-lived radium isotopes (^{226}Ra and ^{228}Ra) stabilizes. The shelf region has longer water residence times (years) and/or deeper water reaching the shelf break (< 200 m).

To estimate SGD, we first obtained fluxes from all radium and radon sources and sinks except for SGD. The difference in all sources and sinks was assumed to represent the radium or radon flux derived from multiple SGD pathways[3,42,67,68]. The source terms of isotopes included river input (both dissolved and desorbed from particles), sediment diffusion, atmospheric deposition, and the ingrowth from their parent isotopes. The sink terms were decay loss, mixing and atmospheric loss. The combined mass balance models of ^{222}Rn and ^{224}Ra were used to distinguish the two unknowns: the nearshore-scale FSGD and RSGD. Based on mass balances of ^{226}Ra and ^{228}Ra, the shelf-scale RSGD can be compared with nearshore-scale RSGD, providing insights into groundwater-seawater exchange across the shelf. Additional details appear in Supplementary Note 1. A Monte Carlo simulation was applied to resolve uncertainties and the most likely fluxes on a MATLAB platform (version MATLAB R2018a). The results of Monte Carlo simulations are inherently stochastic, even with the same model and parameters. In order to verify the robustness of the results, we performed ten simulations and statistically analyze the results. The stochastic uncertainties were respectively ~4% and 3–9% of the overall uncertainties of the multi-scale estimates of FSGD and RSGD. The main conclusions thus persist without a major impact of stochastic uncertainties.

Data availability

Source data are provided with this paper in Supplementary Data 1. The input data for Monte Carlo simulations and the mass balance models in this study are provided in the Supplementary Information and Supplementary Data 2.

Code availability

The code used in this study are available at: https://doi.org/10.5281/zenodo.14891255.

References

1. Burnett, W. C., Bokuniewicz, H., Huettel, M., Moore, W. S. & Taniguchi, M. Groundwater and pore water inputs to the coastal zone. *Biogeochemistry* **66**, 3–33 (2003).
2. Moore, W. S. The effect of submarine groundwater discharge on the ocean. *Annu. Rev. Mar. Sci.* **2**, 59–88 (2010).
3. Moore, W. S. Large groundwater inputs to coastal waters revealed by Ra-226 enrichments. *Nature* **380**, 612–614 (1996).
4. Michael, H. A., Mulligan, A. E. & Harvey, C. F. Seasonal oscillations in water exchange between aquifers and the coastal ocean. *Nature* **436**, 1145–1148 (2005).
5. Luijendijk, E., Gleeson, T. & Moosdorf, N. Fresh groundwater discharge insignificant for the world's oceans but important for coastal ecosystems. *Nat. Commun.* **11**, 1260 (2020).
6. Santos, I. R. et al. Submarine groundwater discharge impacts on coastal nutrient biogeochemistry. *Nat. Rev. Earth Environ.* **2**, 307–323 (2021).
7. Moore, W. S., Sarmiento, J. L. & Key, R. M. Submarine groundwater discharge revealed by ^{228}Ra distribution in the upper Atlantic Ocean. *Nat. Geosci.* **1**, 309–311 (2008).
8. Adyasari, D. et al. Radon-222 as a groundwater discharge tracer to surface waters. *Earth-Sci. Rev.* **238**, 104321 (2023).
9. Garcia-Orellana, J. et al. Radium isotopes as submarine groundwater discharge (SGD) tracers: review and recommendations. *Earth-Sci. Rev.* **220**, 103681 (2021).
10. Rodellas, V., Garcia-Orellana, J., Masqué, P., Feldman, M. & Weinstein, Y. Submarine groundwater discharge as a major source of nutrients to the Mediterranean Sea. *Proc. Natl Acad. Sci. U.S.A.* **112**, 3926–3930 (2015).
11. Wilson, S. J. et al. Global subterranean estuaries modify groundwater nutrient loading to the ocean. *Limnol. Oceanogr. Lett.* **9**, 411–422 (2024).
12. McKenzie, T. et al. Metals in coastal groundwater systems under anthropogenic pressure: a synthesis of behavior, drivers, and emerging threats. *Limnol. Oceanogr. Lett.* **9**, 388–410 (2024).
13. Tomer, A. S. et al. Groundwater releases CO_2 to diverse global coastal ecosystems. *Sci. Adv.* **11**, eadr3240 (2025).
14. Wang, B., Xin, M., Wei, Q. & Xie, L. A historical overview of coastal eutrophication in the China Seas. *Mar. Pollut. Bull.* **136**, 394–400 (2018).
15. Howarth, R. W. Coastal nitrogen pollution: a review of sources and trends globally and regionally. *Harmful Algae* **8**, 14–20 (2008).
16. Liu, S., Hong, G.-H., Zhang, J., Ye, X. W. & Jiang, X. L. Nutrient budgets for large Chinese estuaries. *Biogeosciences* **6**, 2245–2263 (2009).
17. Dai, Z., Du, J., Zhang, X., Su, N. & Li, J. Variation of riverine material loads and environmental consequences on the Changjiang

(Yangtze) estuary in recent decades (1955-2008). *Environ. Sci. Technol.* **45**, 223–227 (2011).
18. Chen, C.-T. A., Wang, S.-L., Wang, B.-J. & Pai, S.-C. Nutrient budgets for the South China Sea basin. *Mar. Chem.* **75**, 281–300 (2001).
19. Wu, S. et al. Nitrogen cycling in China marginal seas: progress and challenges. *Mar. Chem.* **265–266**, 104421 (2024).
20. Liu, J. et al. Distribution and budget of dissolved and biogenic silica in the Bohai Sea and Yellow Sea. *Biogeochemistry* **130**, 85–101 (2016).
21. Wang, J. et al. Spatially explicit inventory of sources of nitrogen inputs to the Yellow Sea, East China Sea, and South China Sea for the Period 1970–2010. *Earth's. Future* **8**, e2020EF001516 (2020).
22. Ren, W., Ji, J., Chen, L. & Zhang, Y. Evaluation of China's marine economic efficiency under environmental constraints—an empirical analysis of China's eleven coastal regions. *J. Clean. Prod.* **184**, 806–814 (2018).
23. Westberry, T. K., Silsbe, G. M. & Behrenfeld, M. J. Gross and net primary production in the global ocean: an ocean color remote sensing perspective. *Earth-Sci. Rev.* **237**, 104322 (2023).
24. Zhang, Y. et al. Submarine groundwater discharge drives coastal water quality and nutrient budgets at small and large scales. *Geochimica et. Cosmochimica Acta* **290**, 201–215 (2020).
25. Yu, X., Liu, J., Wang, X., Chen, X. & Du, J. Unveiling the dominance of submarine groundwater discharge on nutrient sources in the Eastern China Marginal Seas. *Water Res.* **262**, 122136 (2024).
26. Cho, H.-M. et al. Radium tracing nutrient inputs through submarine groundwater discharge in the global ocean. *Sci. Rep.* **8**, 2439 (2018).
27. Santos, I. R., Eyre, B. D. & Huettel, M. The driving forces of porewater and groundwater flow in permeable coastal sediments: a review. *Estuar., Coast. Shelf Sci.* **98**, 1–15 (2012).
28. Fu, Y., Chen, Y. & Zhang, Z. Temporal and spatial variation of population density of coastal cities during 1985-2010 in China (in Chinese). *Tropical Geogr.* **34**, 635–642 (2014).
29. Liu, X. et al. Simulating water residence time in the coastal ocean: a global perspective. *Geophys. Res. Lett.* **46**, 13910–13919 (2019).
30. Luo, C. et al. Seasonal variations in the water residence time in the Bohai Sea using 3D hydrodynamic model study and the adjoint method. *Ocean Dyn.* **71**, 157–173 (2021).
31. Men, W. & Liu, G. Distribution of ^{226}Ra and the residence time of the shelf water in the Yellow Sea and the East China Sea. *J. Radioanal. Nucl. Chem.* **303**, 2333–2344 (2015).
32. Liu, K., Atkinson, L., Quinones, R. & Talaue-McManus, L. *Carbon and Nutrient Fluxes in Continental Margins: A Global Synthesis*. (Springer Berlin, Heidelberg, 2010).
33. Zhao, S. et al. Nutrient-rich submarine groundwater discharge fuels the largest green tide in the world. *Sci. Total Environ.* **770**, 144845 (2021).
34. Liu, J., Du, J., Wu, Y. & Liu, S. Nutrient input through submarine groundwater discharge in two major Chinese estuaries: the Pearl River Estuary and the Changjiang River Estuary. *Estuar., Coast. Shelf Sci.* **203**, 17–28 (2018).
35. Guimond, J. A., Seyfferth, A. L., Moffett, K. B. & Michael, H. A. A physical-biogeochemical mechanism for negative feedback between marsh crabs and carbon storage. *Environ. Res. Lett.* **15**, 034024 (2020).
36. Xin, P. et al. Surface water and groundwater interactions in salt marshes and their impact on plant ecology and coastal biogeochemistry. *Rev. Geophysics* **60**, e2021RG000740 (2022).
37. Chen, X. et al. Submarine groundwater-borne nutrients in a tropical bay (Maowei Sea, China) and their impacts on the oyster aquaculture. *Geochem. Geophys. Geosyst.* **19**, 932–951 (2018).
38. Tang, G., Yi, L., Liu, L. & Cheng, X. Factors influencing the distribution of ^{223}Ra and ^{224}Ra in the coastal waters off Tanggu and Qikou in Bohai bay. *Continental Shelf Res.* **109**, 177–187 (2015).
39. Moore, W. S. Radium isotopes in the Chesapeake Bay. *Estuar., Coast. Shelf Sci.* **12**, 713–723 (1981).
40. Gonneea, M. E., Morris, P. J., Dulaiova, H. & Charette, M. A. New perspectives on radium behavior within a subterranean estuary. *Mar. Chem.* **109**, 250–267 (2008).
41. Webster, I. T., Hancock, G. J. & Murray, A. S. Modelling the effect of salinity on radium desorption from sediments. *Geochimica et. Cosmochimica Acta* **59**, 2469–2476 (1995).
42. Burnett, W. C. & Dulaiova, H. Estimating the dynamics of groundwater input into the coastal zone via continuous radon-222 measurements. *J. Environ. Radioactivity* **69**, 21–35 (2003).
43. Vinson, D. S. et al. Occurrence and mobilization of radium in fresh to saline coastal groundwater inferred from geochemical and isotopic tracers (Sr, S, O, H, Ra, Rn). *Appl. Geochem.* **38**, 161–175 (2013).
44. Xu, B. et al. Closing the global marine ^{226}Ra budget reveals the biological pump as a dominant removal flux in the upper ocean. *Geophysical Research Letters* **49**, e2022GL098087 (2022).
45. Liu, J., Du, J. & Yi, L. Ra tracer-based study of submarine groundwater discharge and associated nutrient fluxes into the Bohai Sea, China: a highly human-affected Marginal Sea: nutrient fluxes via SGD into Bohai Sea. *J. Geophys. Res. Oceans* **122**, 8646–8660 (2017).
46. Zhang, X. et al. A comprehensive analysis of submarine groundwater discharge and nutrient fluxes in the Bohai Sea, China. *Water Res.* **253**, 121320 (2024).
47. Liu, J., Du, J. & Yu, X. Submarine groundwater discharge enhances primary productivity in the Yellow Sea, China: Insight from the separation of fresh and recirculated components. *Geosci. Front.* **12**, 101204 (2021).
48. Burnett, W. C. et al. Quantifying submarine groundwater discharge in the coastal zone via multiple methods. *Sci. Total Environ.* **367**, 498–543 (2006).
49. Kwon, E. Y. et al. Global estimate of submarine groundwater discharge based on an observationally constrained radium isotope model. *Geophys. Res. Lett.* **41**, 8438–8444 (2014).
50. Micallef, A. et al. Offshore freshened groundwater in continental margins. *Rev. Geophysics* **59**, e2020RG000706 (2021).
51. Post, V. E. A. et al. Offshore fresh groundwater reserves as a global phenomenon. *Nature* **504**, 71–78 (2013).
52. Luo, M. et al. Effect of submarine groundwater discharge on nutrient distribution and eutrophication in Liaodong Bay, China. *Water Res.* **247**, 120732 (2023).
53. Taniguchi, M. et al. Submarine groundwater discharge: updates on its measurement techniques, geophysical drivers, magnitudes, and effects. *Front. Environ. Sci.* **7**, 141 (2019).
54. Xu, G. et al. How does urban population density decline over time? an exponential model for Chinese cities with international comparisons. *Landsc. Urban Plan.* **183**, 59–67 (2019).
55. Zhang, X. & Ning, J. Land use change in coastal zones of China from 1985 to 2020. *Front. Mar. Sci.* **11** https://doi.org/10.3389/fmars.2024.1323032 (2024).
56. Anderson, D. M., Glibert, P. M. & Burkholder, J. M. Harmful algal blooms and eutrophication: nutrient sources, composition, and consequences. *Estuaries* **25**, 704–726 (2002).
57. Wang, J. et al. Harmful algal blooms in chinese coastal waters will persist due to perturbed nutrient ratios. *Environ. Sci. Technol. Lett.* **8**, 276–284 (2021).
58. Chen, C., Liang, J., Yang, G. & Sun, W. Spatio-temporal distribution of harmful algal blooms and their correlations with marine hydrological elements in offshore areas, China. *Ocean Coast. Manag.* **238**, 106554 (2023).
59. Zhao, C., Zang, J., Liu, J., Sun, T. & Ran, X. Distribution and budget of nitrogen and phosphorus and their influence on the ecosystem in

the Bohai Sea and Yellow Sea (in Chinese). *China Environ. Sci.* **36**, 2115–2127 (2016).
60. Ma, Y., Zhang, L., Liu, S. & Zhu, D. Silicon balance in the South China Sea. *Biogeochemistry* **157**, 327–353 (2022).
61. Paytan, A. & Mclaughlin, K. The oceanic phosphorus cycle. *Chem. Rev.* **107**, 563–576 (2007).
62. Slomp, C. P., Malschaert, J. F. P. & Van Raaphorst, W. The role of adsorption in sediment-water exchange of phosphate in North Sea continental margin sediments. *Limnol. Oceanogr.* **43**, 832–846 (1998).
63. Wang, G., Han, A., Chen, L., Tan, E. & Lin, H. Fluxes of dissolved organic carbon and nutrients via submarine groundwater discharge into subtropical Sansha Bay, China. *Estuar., Coast. Shelf Sci.* **207**, 269–282 (2018).
64. Wang, Y. et al. Long-term nutrient variation trends and their potential impact on phytoplankton in the southern Yellow Sea, China. *Acta Oceanol. Sin.* **41**, 54–67 (2022).
65. Xin, M. et al. Long-term changes in nutrient regimes and their ecological effects in the Bohai Sea, China. *Mar. Pollut. Bull.* **146**, 562–573 (2019).
66. Chen, X., Wang, J., Cukrov, N. & Du, J. Porewater-derived nutrient fluxes in a coastal aquifer (Shengsi Island, China) and its implication. *Estuar., Coast. Shelf Sci.* **218**, 204–211 (2019).
67. Hwang, D.-W., Kim, G., Lee, Y.-W. & Yang, H.-S. Estimating submarine inputs of groundwater and nutrients to a coastal bay using radium isotopes. *Mar. Chem.* **96**, 61–71 (2005).
68. Kim, G., Ryu, J.-W., Yang, H.-S. & Yun, S.-T. Submarine groundwater discharge (SGD) into the Yellow Sea revealed by ^{228}Ra and ^{226}Ra isotopes: Implications for global silicate fluxes. *Earth Planet. Sci. Lett.* **237**, 156–166 (2005).
69. Liu, S., Li, L. & Zhang, Z. Inventory of nutrients in the Bohai. *Continental Shelf Res.* **31**, 1790–1797 (2011).
70. Wang, Q. et al. Submarine groundwater discharge and its implication for nutrient budgets in the western Bohai Bay, China. *J. Environ. Radioactivity* **212**, 106132 (2020).

Acknowledgements

We would like to thank Xiaoyi Guo, Disong Yang, Haiming Nan, Han Zhang, Haowei Xu, Lijun Song, Wen Liu, Miaomiao Zhang for their assistance during sample collection. We would like to thank Jianing Zhang and Shasha Song for their assistance during model establishing. This work is funded by Natural Science Foundation of China (NSFC grant 42425602 to B.X., 42130410 to Z.Y., 42030402 to D.L., and U22A20580 to B.X.). Data and samples were collected onboard of R/V "Runjiang 1" "Lanhai 201" "Kexue 3" "Bohaike" implementing the open research cruises NORC2021-03, NORC2022-03, NORC2023-03 + NORC2023-302 supported by NSFC ship time Sharing Project (project number: 42049903, 42149903, 42249903). We would like to thank High-End Foreign Experts Recruitment Plan of China (G2023151003L to B.X.).

Author contributions

B.X. and Z.Y. designed the research. T.Z. wrote the initial draft with close input from B.X., I.R.S., and M.B.C. T.Z. collected the data in China marginal seas and adjacent coastal areas with the help from D.L., Y.Z., X.C., L.Y., H-M.C., S.L., S.Z. and G.C. I.R.S., S.Z., B.X. and W.C.B. helped with the further language editing and designing the manuscript. M.B.C. helped with the Monte Carlo simulation. H.Y. and Z.Z. constructed the Lagrangian model for water age estimations and supported writing of the related section. X.C., K.X., and E.L. helped with the figures. B.X. and Z.Y. secured funding for this study. All authors edited the manuscript, provided suggestions, and agree with submission.

Competing interests

The authors declare no competing interests.

Additional information

Supplementary information The online version contains supplementary material available at https://doi.org/10.1038/s41467-025-58103-y.

Correspondence and requests for materials should be addressed to Bochao Xu or Zhigang Yu.

Peer review information *Nature Communications* thanks Xiaolang Zhang and the other, anonymous, reviewer(s) for their contribution to the peer review of this work. A peer review file is available.

[1]Frontiers Science Center for Deep Ocean Multispheres and Earth System, and Key Laboratory of Marine Chemistry Theory and Technology, Ministry of Education, Ocean University of China, Qingdao 266100, P. R. China. [2]Laboratory for Marine Ecology and Environmental Science, Qingdao Marine Science and Technology Center, Qingdao 266100, P. R. China. [3]College of Chemistry and Chemical Engineering, Ocean University of China, Qingdao 266100, P. R. China. [4]Academy of Future Ocean, Ocean University of China, Qingdao 266100, P. R. China. [5]State Key Laboratory of Estuarine and Coastal Research, Institute of Eco-Chongming, East China Normal University, Shanghai 200241, P. R. China. [6]University of Texas at Austin, Austin, Texas, USA. [7]College of Oceanic and Atmospheric Sciences, Ocean University of China, Qingdao 266100, P. R. China. [8]Sanya Oceanographic Institution, Ocean University of China, Sanya 572000, P. R. China. [9]MOE Key Laboratory of Groundwater Circulation and Environment Evolution, School of Water Resources and Environment, China University of Geosciences (Beijing), Beijing 100083, P. R. China. [10]Key Laboratory of Coastal Environment and Resources of Zhejiang Province, School of Engineering, Westlake University, Hangzhou 310024, P. R. China. [11]CAS Key Laboratory of Coastal Environmental Processes and Ecological Remediation, Yantai Institute of Coastal Zone Research, Chinese Academy of Sciences, Yantai 264003, P. R. China. [12]College of Environmental Science and Engineering, Nankai University, 94 Weijin Rd, Tianjin, P. R. China. [13]Department of Ocean Sciences, Inha University, Incheon 22212, Republic of Korea. [14]Qingdao Collaborative Innovation Center

of Marine Science and Technology, Qingdao, P. R. China. [15]Ecological Environment Monitoring and Scientific Research Center, Taihu Basin & East China Sea Ecological Environment Supervision and Administration Bureau, Ministry of Ecology and Environment, Shanghai 200125, P. R. China. [16]State Key Laboratory of Marine Geology, Tongji University, Shanghai 200092, P. R. China. [17]Department of Earth, Ocean and Atmospheric Science, Florida State University, Tallahassee, FL 32306, USA. [18]First Institute of Oceanography, Ministry of Natural Resources, Qingdao 266061, P. R. China. [19]Department of Marine Sciences, University of Gothenburg, Gothenburg 41319, Sweden. ✉e-mail: xubc@ouc.edu.cn; zhigangyu@ouc.edu.cn